5
Reconfigurable UWB Antenna

The growing demand in wireless communication requires compact wideband/multiband antennas with reconfigurable characteristics to utilize the spectrum efficiently. Antenna, being the front end its dimension must be compact to have portable communication systems. However, UWB band faces the electromagnetic interference problems with some existing narrowband communication systems such as WiMAX in 3.3-3.8 GHz, WLAN in 5.15-5.85 GHz and X-band in 7.9-8.4 GHz. In case of no interference scenario, UWB bandwidth is not utilized efficiently. Therefore, there is a need of reconfigurable band reject UWB antenna to exploit the frequency spectrum efficiently. Wideband antennas with narrowband reconfigurability are suitable candidates for software-defined radio (SDR) and cognitive radio (CR) applications, to sense the wideband frequency spectrum and then communicate through narrowband frequency spectrum. The SDR uses reconfigurable modulation scheme, whereas CR has the features of software-defined radio with artificial intelligence which helps in sensing the free frequency spectrum and then take the appropriate decision for transmission. Thus, CR system requires an antenna which has the wideband sensing capability as well as narrowband transmission reconfigurability. Hence, design of reconfigurable antennas, which have reconfigurable band notch characteristics or reconfigurable narrowband characteristics, are required. The objective of this chapter is to incorporate reconfigurable functionality in antenna while keeping its footprint small. Based on this, to verify the reconfigurability in interference band and operational band, two antennas are designed and respective concepts are verified through fabrication and measurements.

5.1 Introduction

The UWB communication systems get the researchers attention due to its inherent properties such as wideband, low profile, low power transmission, high data transmission capacity, omnidirectional radiation pattern, and easy fabrication. The commercial application of UWB technology requires compactness in antenna design, so that, it can be integrated easily with portable devices. The developments in wireless communication system with increasing demand for frequency bands to facilitate voice, data and video services have created the spectrum scarcity due to Fixed Spectrum Access (FSA) policy of regulatory authorities. However, most of the time, the allocated spectrum remain idle. It is due to inefficient use of spectrum at irregular intervals of time. In order to utilize the spectrum efficiently, Dynamic Spectrum Access (DSA) based CR technology is proposed. It requires a sensing antenna to monitor the system as well as a communicating antenna which can be reconfigured to transfer the data in the selected spectrum [Mitola, 1999].

However, UWB band faces the interferences with the existing narrowband communication systems. In order to overcome the above challenges, several UWB antennas with band notch characteristics are presented [Peng *et al.*, 2013; Abdollahvand *et al.*, 2010; Azim *et al.*, 2014]. However, these antennas are not able to utilize the UWB band effectively in case of no interference issues. Thus, the design of UWB antenna with reconfigurable single/dual band notch characteristics is desirable. In [Valizade *et al.*, 2012] and [Badamchi *et al.*, 2014], the reconfigurable band notch antenna are presented and they are large in size. In addition, the

researchers have proposed to integrate sensing and narrowband communication in the UWB band [Erfani *et al.*, 2012; Boudaghi *et al.*, 2012; Ebrahimi *et al.*, 2011; Tawk *et al.*, 2011; Zamudio *et al.*, 2011]. In [Erfani *et al.*, 2012] and [Boudaghi *et al.*, 2012], varactor diodes and p-i-n diodes are used for reconfigurable narrowband within the UWB band, respectively. A planar inverted-F resonator on the back side of the antenna is proposed to have reconfigurability in antenna design [Ebrahimi *et al.*, 2011]. The stepper motor is used to rotate the circular part and achieve a narrowband operating frequency for each rotation [Tawk *et al.*, 2011]. Whereas, reconfigurable band pass filter is incorporated in UWB antenna to get narrowband reconfigurability [Zamudio *et al.*, 2011]. However, these antennas are large in dimensions and complex in design, which leads to increase the cost of the systems. The commercial applications of UWB technology require compactness in antenna dimensions, so that; it can be easily integrated with other portable devices.

Therefore, to achieve the compactness as well as wideband characteristics in the antenna design, fractal geometry is used because of its self-similar and space filling properties [Werner *et al.*, 1999; Anguera *et al.*, 2005; Hashemi *et al.*, 2006]. The space filling property of fractal geometry leads to enhance the effective electrical path length of the antenna in a given smaller area, whereas self-similar phenomena generates multiple resonances, which helps to achieve wideband characteristics [Werner *et al.*, 1999; Anguera *et al.*, 2005]. Some, popular fractal geometries such as Koch snowflake [Anguera *et al.*, 2005], hexagonal shaped [Werner *et al.*, 1999], and Sierpinski triangle [Werner *et al.*, 1999; Anguera *et al.*, 2005] are used in UWB antenna design. In order to achieve the reconfigurable performance in rejection bands, different types of switches such as RF MEMS, RF MESFET, varactor diodes and p-i-n diodes are used. Hence, design of a compact UWB antenna with reconfigurable operating bands as well as reconfigurable band notch characteristics is essential for efficient utilization of UWB spectrum.

5.2 Fractal UWB Antenna with Reconfigurable Band-notch Functions

5.2.1 Antenna Design

(a) Antenna Configuration

In this section, a compact octagonal shaped fractal UWB antenna with triple band notch characteristics is presented. The Sierpinski fractal geometry is applied to achieve miniaturization and wideband in antenna design. The proposed reconfigurable fractal UWB antenna with its design parameters is shown in Figure 5.1. Its design and fabrication is carried out using rectangular FR4 epoxy substrate ($W_{sub} \times L_{sub}$), having a dielectric constant of $\varepsilon_r = 4.4$, loss tangent $\tan\delta = 0.023$, and thickness (h) of 1.6 mm. The presented antenna is simulated and optimized using Ansoft HFSS v.13. The initial dimension of substrate in the evolution of the antenna design is selected as rectangular due to its wide operational bandwidth and good radiation characteristics [Tasouji *et al.*, 1998]. The patch is connected to a 50 Ω microstrip line for impedance matching. The ground plane of the proposed design is situated on the other side of the substrate. The optimised dimensions of the proposed reconfigurable fractal UWB antenna design are: L_{sub} = 24.5 mm, W_{sub} = 20 mm, R = 4.6 mm, W_m = 3.2 mm, L_g = 11 mm, L_s = 2 mm, W_s = 3 mm, L_1 = 3 mm, L_2 = 7 mm, L_3 = 1.2 mm, L_4 = 0.2 mm, L_5 = 2.3 mm, L_6 = 0.5 mm, L_7 = 1.2 mm, L_8 = 1.2 mm, L_9 = 6.4 mm, L_{10} = 9.8 mm, L_{11} = 1.8 mm, L_{12} = 4 mm and L_{13} = 0.25 mm.

In this study, the proposed novel antenna is generated by applying Sierpinski fractal at the edges of octagonal geometry. Figure 5.2 shows the iterative evolution of the Sierpinski fractal. In the evolution process of initial antenna design, the octagonal geometry and Sierpinski geometry works as a initiator and generator, respectively, as shown in Figure 5.3. The return loss variations for different antennas generated in Figure 5.3 are shown in Figure 5.4. Figure 5.3(a) shows the initial iteration-0 geometry without fractal application, whereas Figure 5.3(b) and (c) represents the application of first and second iteration of Sierpinski fractal at the edges of octagonal geometry, respectively. It can be seen from Figure 5.4, that the application of fractal geometry in the design helps to improve the operational bandwidth in the higher operating

band. This iterative process can be continued up to infinite, but fabrication constraints limit us up to two iterations. The introduction of the rectangular slot in the ground plane, etching of two C-shaped slots from FM and introduction of two CSSRR on both sides of feed line in the design is shown in Figure 5.3(d), which helps to obtain multiple notch band characteristics as well as improvement in operating bandwidth. Moreover, the use of fractal geometry in antenna design leads to repetitions of self-similar structure in the geometry. These small segments in the design, excites multiple resonances and by combining them together a wideband operational bandwidth is achieved. Furthermore, the presented reconfigurable UWB antenna has smaller dimensions compared to antennas proposed in [Valizade *et al.*, 2012; Badamchi *et al.*, 2014].

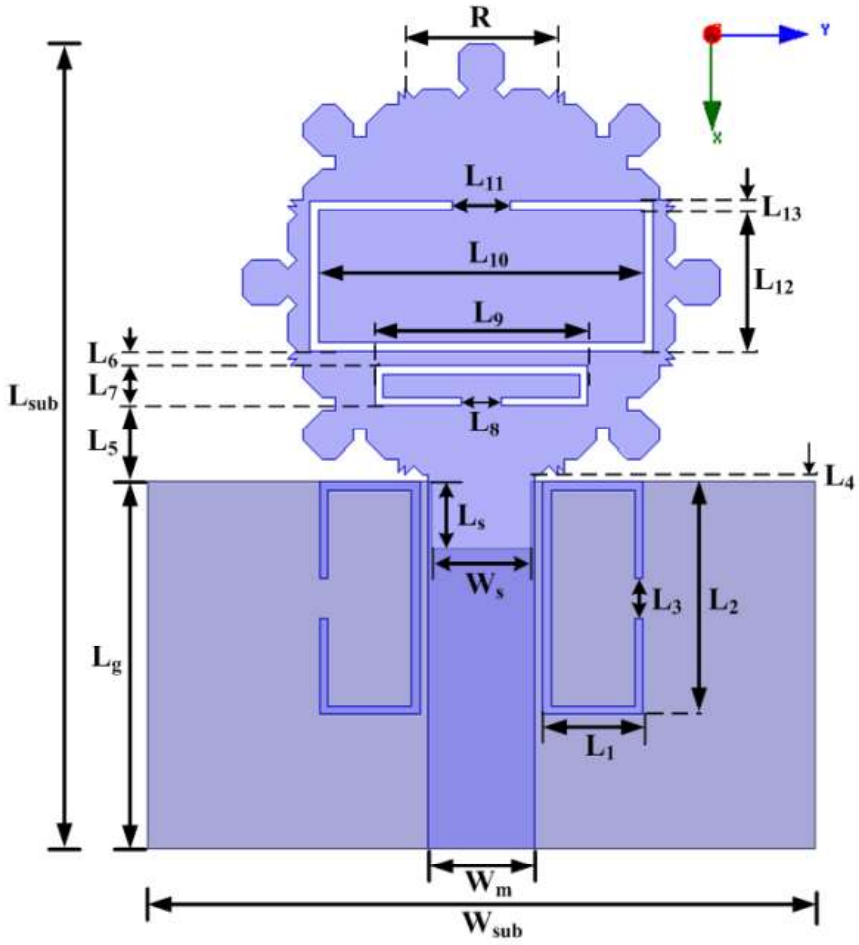

Figure 5.1: Geometry of the proposed reconfigurable fractal UWB antenna

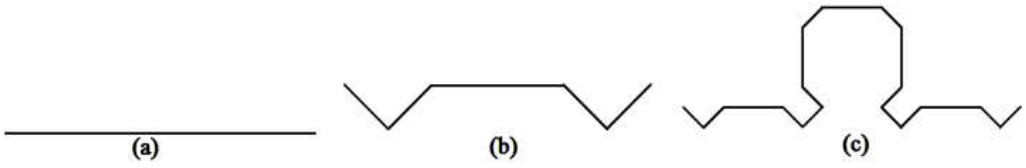

Figure 5.2: Iteration wise generation of Sierpinski geometry (a) Iteration-0, (b) Iteration-1 and (c) Iteration-2

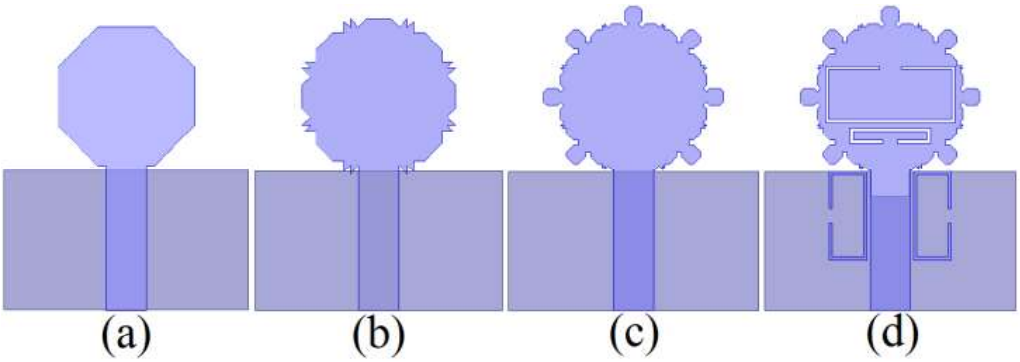

Figure 5.3: Iteration wise evolution of the proposed antenna (a) After iteration-0, (b) After iteration-1, (c) After iteration-2 and (d) Final geometry

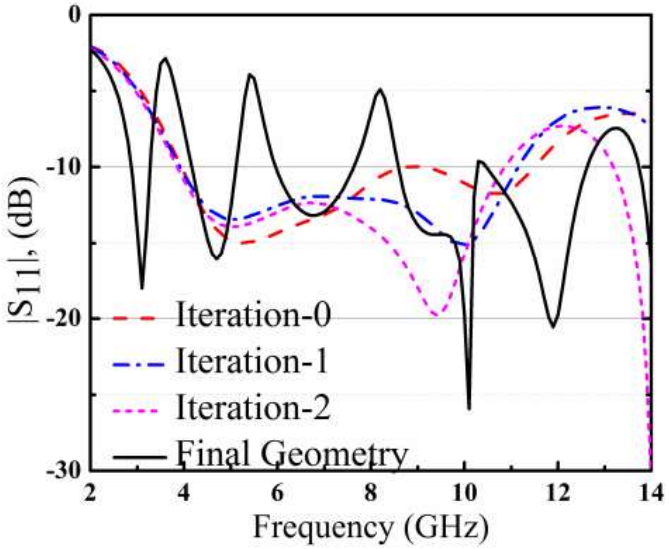

Figure 5.4: Simulated return loss variation of the antennas shown in Figure 5.3

(b) Effect of multiple notch band slots

The triple notch band over WiMAX (3.3-3.8 GHz), WLAN (5.15-5.85 GHz) and X-bands (7.9-8.4 GHz); C-shaped geometries are used in the antenna design. The approximate length of the slot is estimated mathematically using following expression:

$$L_{notch} = \frac{c}{2f_{notch}\sqrt{\varepsilon_{eff}}} \tag{5.1}$$

where c is speed of the light, ε_{eff} is the effective dielectric constant as calculated in [Pozar *et al.*, 1998] and L is the length of the slot. The simulated surface current distributions at notch bands are shown in Figure 5.5 to provide clearer and insight into behavior of the reconfigurable antenna. It can be seen from Figure 5.5(a), (b) and (c) that at notch band current is mainly distributed at the inner and outer edges of C-shaped slot and the direction of surface current is opposite to each other, so they cancel the radiation of each other, which in turn leads to reduction in radiation characteristics/gain of the antenna at notch band frequencies.

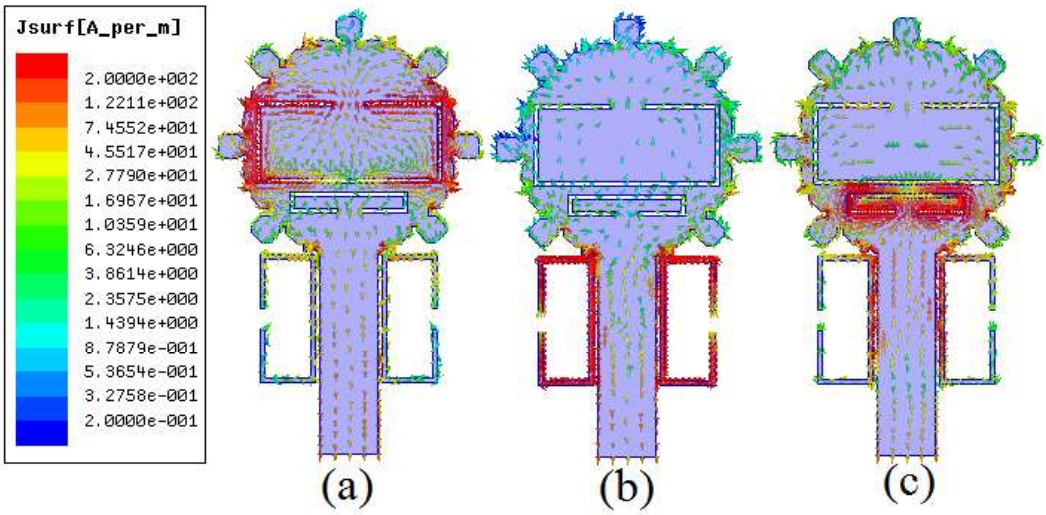

Figure 5.5: Distribution of surface current vector at band notch frequencies (a) 3.7 GHz, (b) 5.5 GHz and (c) 8.2 GHz

In the design process, band rejection in WLAN band and reconfigurability between WiMAX band and X-band are shown due to two reasons. Firstly, WLAN band signals are more prone and present most of the time in UWB spectrum compared to other two interfering signals. Secondly, considering the complexity constraint in the design only dual band reconfigurability is demonstrated. Moreover, the single/dual reconfigurability out of multiple notch band characteristics of the proposed antenna design is achieved by using two BAR 64-04 p-i-n diodes with 100 pF capacitors. These diodes are placed across the middle section of the C-shaped slots to provide an alternative path for current flow, when p-i-n diode is forward biased. These modifications in the geometry help to achieve the single/dual switchable band notch functions, which in turn leads to utilize the UWB band more efficiently, where narrowband interference issues are not present. The capacitor is used in the circuit to create the RF connections as well as isolate the dc from RF signals.

5.2.2 Results and Discussion

(a) VSWR Result

The presented antenna design is fabricated in order to verify the simulated results. Figure 5.6 shows the measured and simulated return loss behaviour of the antenna for different ON/OFF cases of the p-i-n diodes D1 and D2. Diode D1 and D2 are used across C-shaped slots of WLAN and C-band and X-band, respectively. Measurement is performed using E5071C VNA. It can be seen that a good agreement exists between these results. However, some discrepancy is observed due to SMA connectors, soldering effect and substrate quality. Moreover, p-i-n diode and its biasing circuits also affect the results. Besides, the all possible cases of p-i-n diode and corresponding operating bandwidth are shown in Table 5.1. When both the diodes are in ON state, antenna radiates in the UWB band excluding WLAN band. Whereas, in case of both the diodes are OFF, UWB band with triple notch band characteristics are achieved. Meanwhile, in case-3 in which D1 is OFF and D2 is ON, the UWB operating bandwidth with notch band in WiMAX band as well as WLAN band is obtained. Moreover, in case-4 when D1 is ON and D2 is OFF UWB band with notch band in WLAN and X-band is achieved. Therefore, the changes in switching state of p-i-n diode provide the re-configurability among available notch bands in the UWB band.

Table 5.1: Details of p-i-n Diodes Different Cases and Frequency Bands of the Proposed Reconfigurable UWB Antenna

Diodes	D1	D2	Frequency Notch Bands (GHz) Simulated/Measured	
Case-1	ON	ON	5.2-6.0	5.2-5.95
Case-2	OFF	OFF	3.2-4.1, 5.1-5.9, 7.7-8.6	3.2-4.05, 5.1-6.0, 5.95-8.65
Case-3	OFF	ON	3.2-4.1, 5.1-6.0	3.3-4.1, 5.0-6.0
Case-4	ON	OFF	5.2-6.0, 7.6-8.5	5.2-6.05, 7.8-8.4

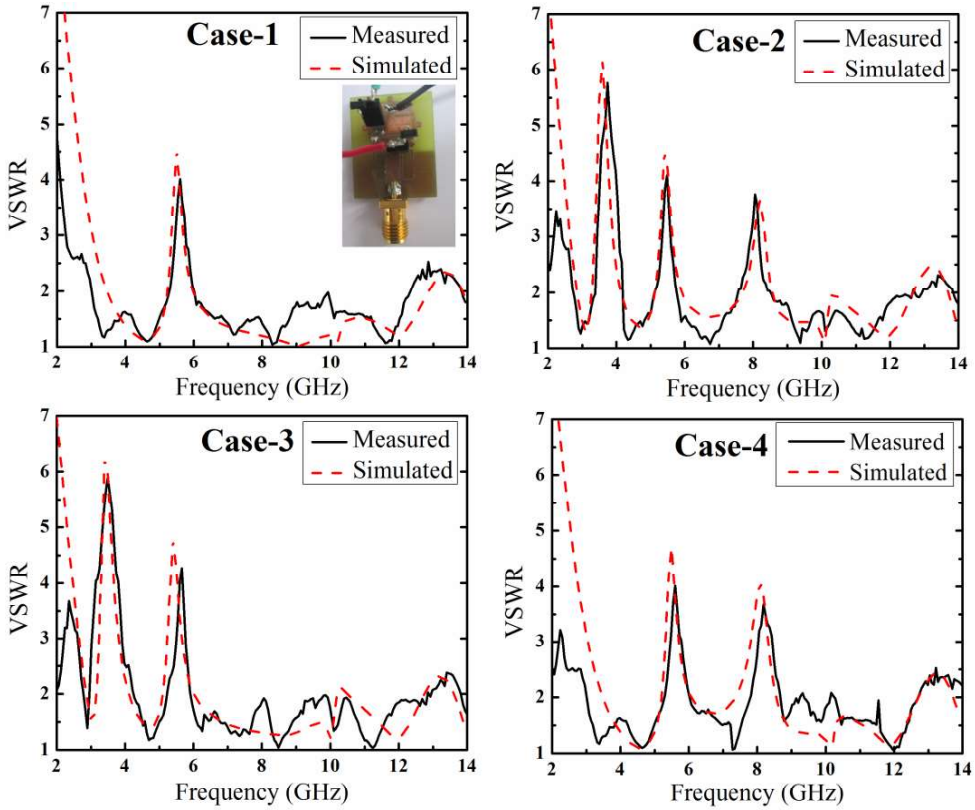

Figure 5.6: Measured and simulated VSWR of the proposed antenna for different reconfigurable cases of Table 5.1

(b) Radiation Performance

The measured radiation pattern of the antenna in E-plane (xz-plane) and H-plane (yz-plane) with co-polarization and cross-polarization, for its quadruple notch band performance is shown in Figure 5.7. As observed, the antenna shows nearly bi-directional behaviour in E-plane and nearly omnidirectional behaviour in H-plane. The radiation pattern at higher resonant frequency is distorted compared to lower resonant frequency because of change in current nature from standing wave pattern at lower frequencies to travelling wave pattern at higher resonant frequencies [Allen *et al.*, 2007]. Figure 5.7 depicts the measured gain of the proposed reconfigurable UWB antenna. It can be seen that gain variation is in the 3 dB range, excluding notch bands. While, in the notch band a significant reduction in gain is observed.

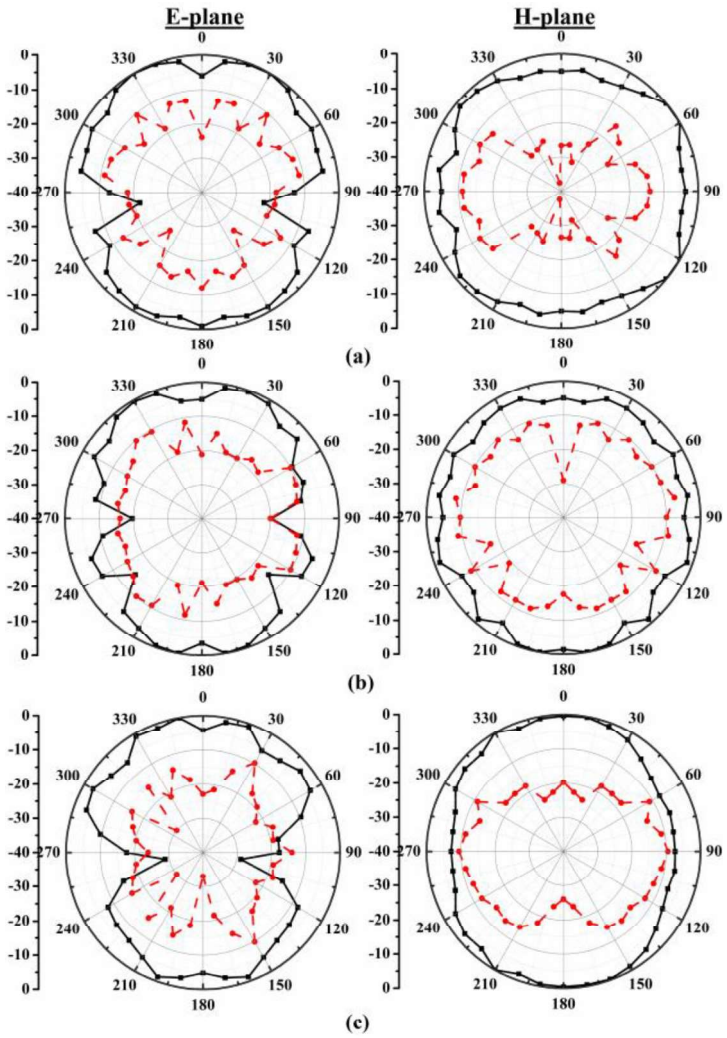

Figure 5.7: Measured radiation pattern of the tested antenna at resonant frequency with co-polarization (—■—) and cross-polarization (— ● —) (a) 4.7 GHz (b) 6.8 GHz and (c) 10.1 GHz

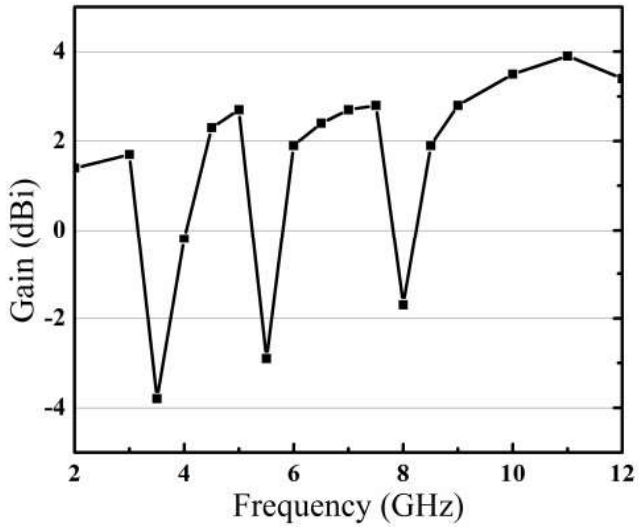

Figure 5.8: Measured gain of the reconfigurable fractal UWB antenna

(c) Time-domain Analysis

In UWB antenna design, time domain characteristic provides a better understanding of antenna performance. The proposed reconfigurable UWB antenna is analyzed in terms of fidelity factor. It predicts the expected distortion produced in the transmitted signal by the antenna. The threshold value of fidelity factor should be more than 0.7 for well matching of radiated pulse with source pulse [Ghuang and Jeng, 2005; Chako *et al.*, 2013]. Table 5.2 shows the fidelity factor variation in the azimuthal plane as well as elevation plane, which lies in the range of 0.71 to 0.94. Therefore it can be concluded that the proposed antenna structure has a good pulse preserving capability because of its efficient design, which makes it a suitable choice for UWB application.

Table 5.2: Fidelity Factor of the Proposed Antenna

Probe positions (x-z plane)	Fidelity Factor	Probe positions (x-y plane)	Fidelity Factor
$\theta = 0^o, \varphi = 0^o$	0.7190	$\varphi = 0^o, \theta = 90^o$	0.8620
$\theta = 30^o, \varphi = 0^o$	0.7530	$\varphi = 30^o, \theta = 90^o$	0.9149
$\theta = 60^o, \varphi = 0^o$	0.9445	$\varphi = 60^o, \theta = 90^o$	0.8666
$\theta = 90^o, \varphi = 0^o$	0.9039	$\varphi = 90^o, \theta = 90^o$	0.8190

5.3 Frequencies Reconfigurable Fractal UWB Antenna Using Reconfigurable Ground

5.3.1 Antenna Design

(a) Antenna Configuration

In order to design a compact antenna, which can work as a spectrum sensor in the UWB band and show reconfigurable operating bands characteristics in the UWB lower-middle-upper bands? In this section, we have selected the previously designed antenna as shown in section 6.2 with switchable ground plane in order to achieve the operational band reconfigurability as shown in Figure 5.9. The design and fabrication of the antenna is carried out on rectangular FR4 epoxy substrate ($W_{sub} \times L_{sub}$), having a dielectric constant of $\varepsilon_r = 4.4$, loss tangent $\tan\delta = 0.023$ with thickness (h) of 1.6 mm. It is simulated and optimized using Ansoft HFSS v.13. The initial dimension of substrate in the evolution of antenna design is selected as rectangular due to two reasons. First, rectangular substrate offer wide operating bandwidth and second it helps to obtain good radiation characteristics [Tasouji *et al.*, 2013]. The fractal monopole (FM) is connected to a 50 Ω microstrip feed line for impedance matching, whereas ground plane of the antenna is placed on the other side of the substrate. The optimised dimensions of the proposed reconfigurable fractal UWB antenna are: L_{sub} = 24.5 mm, W_{sub} = 20 mm, R = 4.6 mm, W_m = 2.6 mm, L_g = 9.5 mm, L_s = 2 mm, W_s = 3 mm, d = 1.7 mm, L_1 = 0.4 mm, L_2 = 4.2 mm, L_3 = 1.8 mm, L_4 = 0.75 mm, L_5 = 1.5 mm, L_6 = 2.75 mm, and L_7 = 2 mm.

(b) Effect of multiple slots in the ground plane

The reconfigurability among UWB band, lower UWB band, middle UWB band and dual band (lower and higher UWB band) is achieved by using multiple BAR 64-04 p-i-n diodes with 100 pF capacitors in the ground plane at positions shown in Figure 5.10. The application of these diodes across the slot at different places provides an alternative path for current flow, when p-i-n diode is forward biased. These modifications in the geometry provide operational band reconfigurability in the UWB band, which helps to utilize the UWB band more efficiently. The capacitor is used with the p-i-n diode in the circuit to create the RF connections as well as isolate the dc from RF signals.

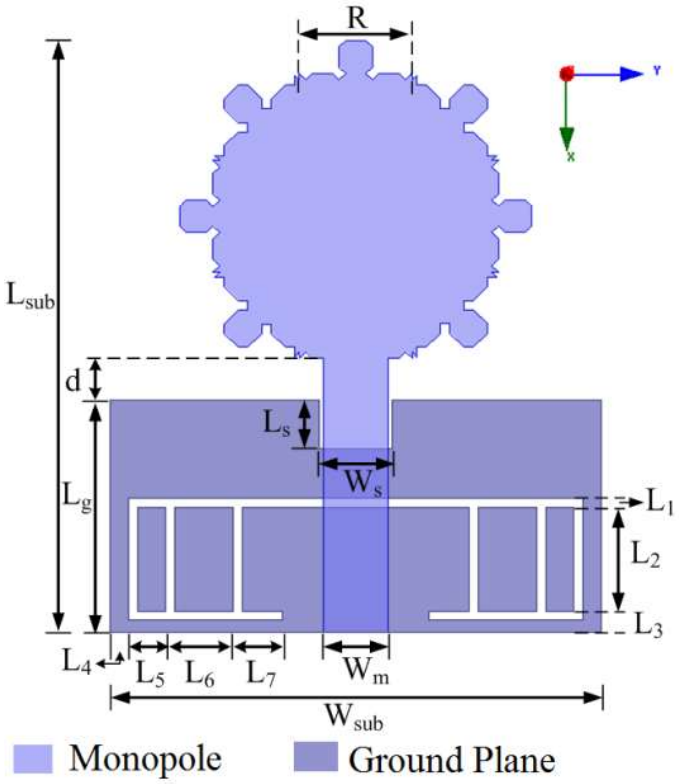

Figure 5.9: Geometry of the proposed reconfigurable fractal UWB antenna

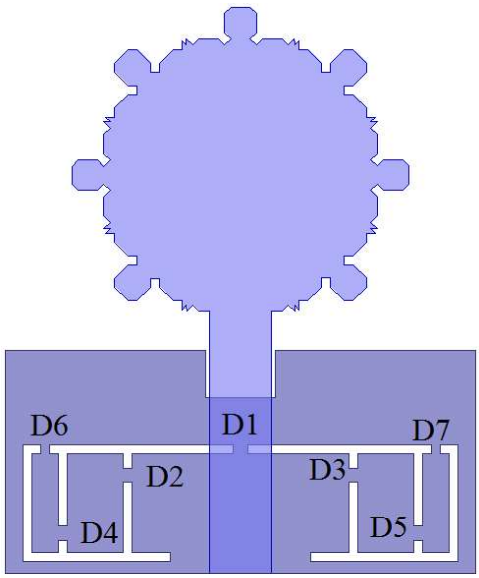

Figure 5.10: Positions of p-i-n diodes in the ground plane of the presented antenna for switching states

Figure 5.11 shows the slotted ground plane structure. The positions of the slots in the ground plane helps to achieve the reconfigurability in the UWB band and are placed at such positions that it creates stopband as well as passband in the UWB bands. The return loss

variations for different antennas generated in Figure 5.11 are shown in Figure 5.12. Figure 5.11(a) shows the initial geometry of the proposed design, which operating bandwidth covers the entire UWB spectrum from 3.1-10.6 GHz. Figure 5.11(b) and (c) shows the introduction position of slot in the ground plane, that helps to achieve passband in lower UWB band and middle UWB band, respectively. While, slot introduced in the Figure 5.11(d) provide dual band passband in lower and higher UWB band. It can be seen from Figure 5.12 that operational bandwidth in UWB band can be controlled easily by changing the length and positions of the slot in the ground plane. The presented antenna, which possesses reconfigurable operating bands, has smaller dimensions as well as simple structure compared to antennas in [Erfani *et al.*, 2012; Boudaghi *et al.*, 2012; Ebrahimi *et al.*, 2011; Tawk *et al.*, 2011; Zamudio *et al.*, 2011]. The performance of antenna is further illustrated using simulated surface current distribution at 4.1 and 8.2 GHz resonant frequencies as shown in Figure 5.13. At lower resonant frequency surface current is distributed at feed line, ground below feed line and some fractal edges of FM, whereas, at higher resonant frequency surface current distribution at fractal edges is enhanced significantly. This improvement in surface current distribution leads to enhance the radiation characteristics at higher frequencies.

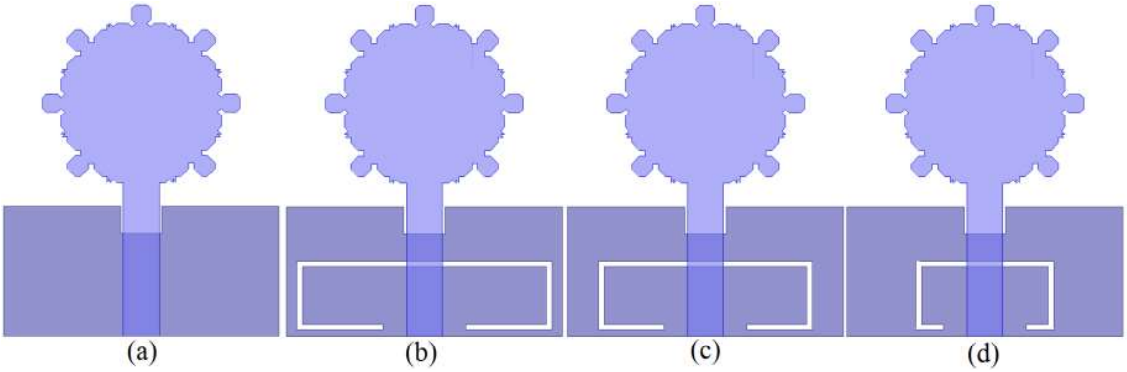

Figure 5.11: Evolution of the proposed antenna (a) Antenna-1, (b) Antenna-2, (c) Antenna-3 and (d) Antenna-4

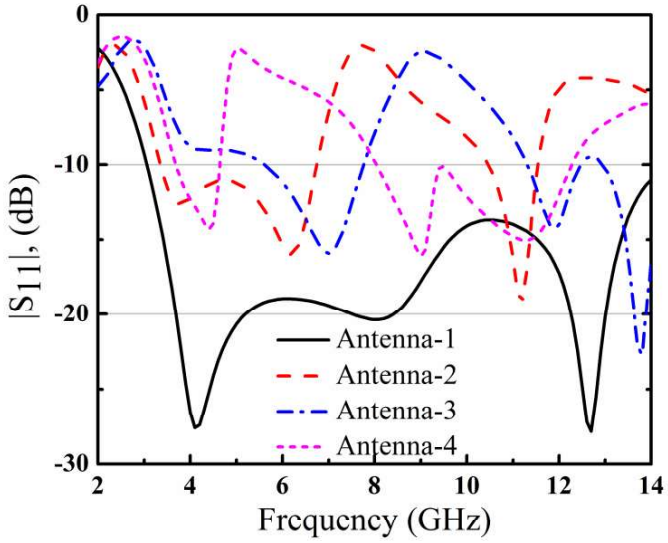

Figure 5.12: Simulated return loss variation of the antennas shown in Figure 5.11

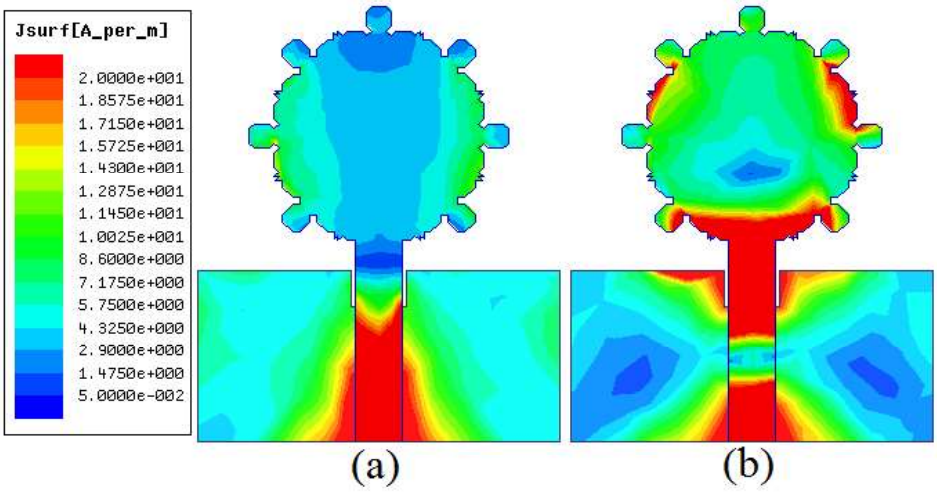

Figure 5.13: Distribution of surface current vector at band notch frequencies (a) 4.1 GHz and (b) 8.2 GHz

5.3.2 Results and Discussion

(a) S-parameter Result

The presented reconfigurable antenna design is fabricated in order to validate the simulated results. Figure 5.14 shows the measured and simulated return loss behaviour of the antenna for different ON/OFF cases of the p-i-n diodes. Some of the possible cases with corresponding operating bandwidth are shown in Table 5.3. Measurement is performed using E5071C vector network analyser (VNA). It can be seen that a good agreement exists between measured and simulated results. However, some discrepancy is observed due to SMA connectors, soldering effect and substrate quality. Furthermore, p-i-n diode and its biasing circuits also affect the results. When all the diodes are in ON state, antenna radiates in the UWB band. Whereas, using the case-II, case-III and case-IV reconfigurable single/dual band in UWB operating band is obtained. Therefore, the variations in switching state of p-i-n diode help to achieve reconfigurability among available operating bands in the UWB band.

Table 5.3: Details of p-i-n Diodes Different Cases and Frequency Bands of the Proposed Reconfigurable UWB Antenna

Diodes States	D1	D2	D3	D4	D5	D6	D7	Operating Bands (GHz) Simulated/Measured	
Case-I	ON	ON	ON	ON	ON	ON	ON	3-14	3.1-14
Case-II	OFF	ON	ON	ON	ON	OFF	OFF	3.3-6.8	3.5-6.7
Case-III	OFF	ON	ON	OFF	OFF	ON	ON	5.6-7.8	5.7-7.9
Case-IV	OFF	OFF	OFF	ON	ON	ON	ON	3.6-4.7,8-12.3	3.7-4.7, 8-9.5, 10.7-12.5

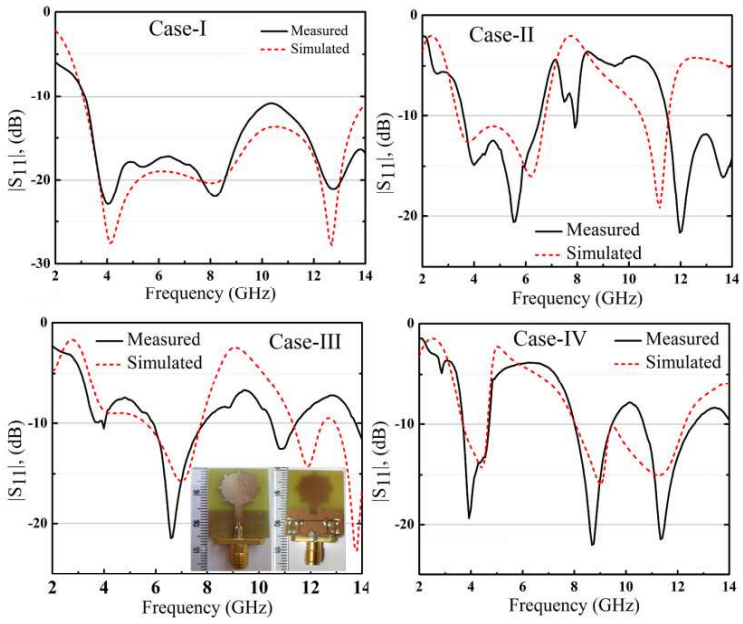

Figure 5.14: Measured and simulated S-parameter of the proposed antenna for different reconfigurable cases of Table 5.3

(b) Radiation Performance

The measured radiation pattern of the reconfigurable UWB antenna in E-plane (xz-plane) and H-plane (yz-plane) with co-polarization and cross-polarization is shown in Figure 5.15. As observed from Figure 5.15 that, the E-plane behavior is nearly bi-directional, whereas H-plane pattern shows nearly omnidirectional behavior. The bends and curves of the fractal structure causes for the change in current path, which in turn leads to enhance the radiation characteristics of the antenna [Balanis, 2005]. Thus, the radiation pattern at higher resonant frequency is not distorted significantly compared to lower resonant frequency irrespective of change in current nature from standing wave pattern at lower frequencies to travelling wave pattern at higher resonant frequencies [Allen *et al.*, 2007]. Figure 5.16 depicts the measured gain of the proposed reconfigurable UWB antenna. It can be seen that gain variation is in the 3 dB range.

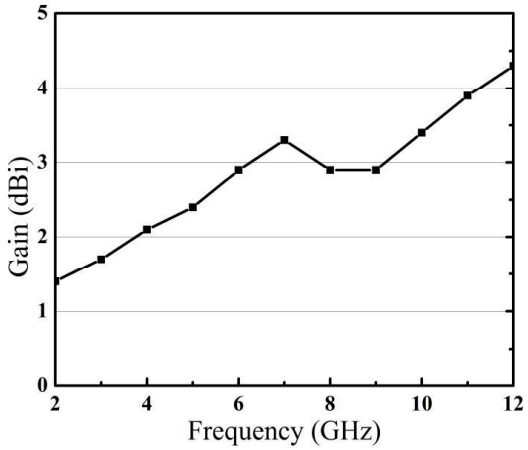

Figure 5.15: Measured gain of the re-configurable fractal UWB antenna

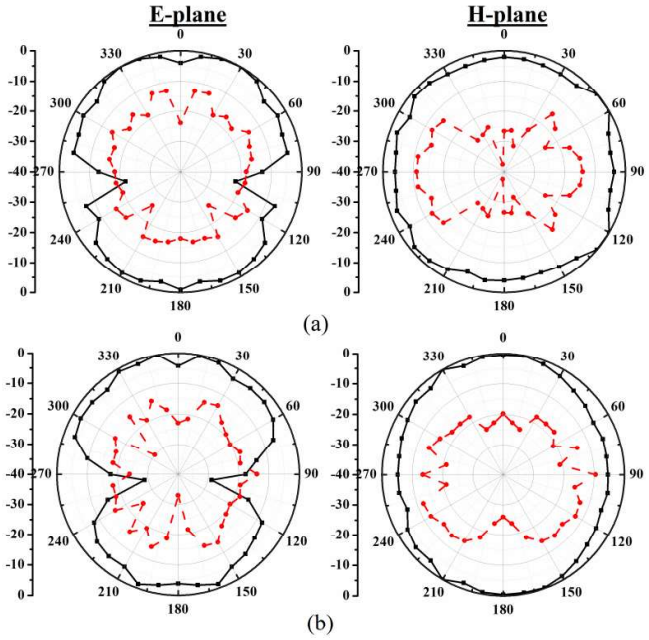

Figure 5.16: Measured radiation pattern of the tested antenna at resonant frequency with co-polarization (—■—) and cross-polarization (— ● —) (a) 4.7 GHz (b) 6.8 GHz and (c) 10.1 GHz

(c) Time-domain Analysis

In UWB antenna design, time domain characteristic provides an insight into behavior of antenna performance. The proposed reconfigurable UWB antenna analysis is carried out in terms of fidelity factor. The virtual probe is defined at a distance of 400 mm for every 30^0 from 0^0 to 90^0. The selected distance should satisfy the far field criteria. In case of well matching of radiated pulse with source pulse the threshold value of fidelity factor should be more than 0.7 [Ghuang and Jeng, 2005; Chako *et al.*, 2013]. The fidelity factor variation in the azimuthal plane as well as elevation plane is shown in Table 5.4. The variation range of fidelity factor is from 0.84 to 0.96. Therefore it can be concluded that the proposed reconfigurable antenna structure has a good pulse preserving capability because of its efficient design.

Table 5.4: Fidelity Factor of the Proposed Antenna

Probe positions (x-z plane)	Fidelity Factor	Probe positions (x-y plane)	Fidelity Factor
$\theta = 0^o, \varphi = 0^o$	0.8490	$\varphi = 0^o, \theta = 90^o$	0.9320
$\theta = 30^o, \varphi = 0^o$	0.8830	$\varphi = 30^o, \theta = 90^o$	0.9649
$\theta = 60^o, \varphi = 0^o$	0.9445	$\varphi = 60^o, \theta = 90^o$	0.9366
$\theta = 90^o, \varphi = 0^o$	0.9439	$\varphi = 90^o, \theta = 90^o$	0.8890

Table 5.5: Comparison of the proposed work with others proposed in the literature

Antenna	Dimensions (mm×mm×mm)	Bandwidth (GHz)	Reconfigurable Bands (GHz)
Work in Section 5.2	24.5×20×1.6	3-12.2	3.3-3.8, 7.9-8.4
Work in Section 5.3	24.5×20×1.6	3-14	3-14,3.3-6.8, 5.6-7.8, (3.6-4.7, 8-12.3)
Boudaghi *et al.*, 2012	40×40×1.6	2.8-10.9	5-6, 3.2-3.8, 2.2-2.8, 2.2-2.8 & 5-5.85
Erfani *et al.*, 2012	40×36×0.66	3-12	4-6
Tawk *et al.*, 2011	65.5×58×1.6	1.5-11	3.4-4.85, 5.3-9.1

5.4 Summary

The application of fractal geometry at the edges of octagonal geometry helps to achieve wide impedance bandwidth. In addition, it provides miniaturization in the design as well as enhances the radiation characteristics. In the first case, a compact reconfigurable UWB antenna with triple notch band characteristics is presented and its properties are investigated. In order to achieve the multiple notch band characteristics two C-shaped slot are etched from the FM and two C-shaped SRR are placed on both sides of feed line. Moreover, to achieve single/dual notch band re-configurability in the design, two p-i-n diodes with 100 pF capacitors are used. The proposed antenna has the compact dimensions of 24.5 mm × 20 mm with good radiation pattern, antenna gain and fidelity factor characteristics. In the second case, a compact reconfigurable UWB antenna with switchable frequency band characteristics is presented. In the proposed design, switchable slotted ground plane is used to provide reconfigurable single/dual bands in the UWB band for CR applications. Single/dual bands reconfigurability is achieved by using multiples p-i-n diodes at different positions of slots in the ground plane, which helps in effective utilization of UWB spectrum. Moreover, proposed antenna shows omnidirectional radiation pattern, acceptable antenna gain with good fidelity factor. A comparison between proposed work in the chapter and the work presented in the literature is also carried out, in the Table 5.5, in terms of antenna dimension, operational bandwidth and reconfigurable bandwidth. Thus, it can be concluded that the proposed antennas are suitable candidate for portable UWB applications.

…